Creating a tunable spin squeezing via a time-dependent collective atom-photon coupling

Lixian Yu,[1,2] Jingtao Fan,[2] Shiqun Zhu,[3] Gang Chen,[2,*] Suotang Jia,[2,†] and Franco Nori[4,5,6,‡]

[1]*Department of Physics, Shaoxing University, Shaoxing 312000, China*

[2]*State Key Laboratory of Quantum Optics and Quantum Optics Devices, Institute of Laser spectroscopy, Shanxi University, Taiyuan 030006, China*

[3]*School of Physical Science and Technology, Soochow University, Suzhou 215006, China*

[4]*CEMS, RIKEN, Saitama 351-0198, Japan*

[5]*Physics Department, The University of Michigan, Ann Arbor, Michigan 48109-1040, USA*

[6]*Department of Physics, Korea University, Seoul 136-713, Korea*

(Received 6 October 2013; published 21 February 2014)

We present an experimentally feasible method to produce a large and tunable spin squeezing when an ensemble of many four-level atoms interacts simultaneously with a single-mode photon and classical driving lasers. Our approach is to simply introduce a time-dependent collective atom-photon coupling. We show that the maximal squeezing factor measured experimentally can be well controlled by both its driving magnitude and driving frequency. In particular, when increasing the driving magnitude, the maximal squeezing factor increases and thus can be rapidly enhanced. We also demonstrate explicitly in the high-frequency approximation that this spin squeezing arises from a strong repulsive spin-spin interaction induced by the time-dependent collective atom-photon coupling. Finally, we evaluate analytically, by using current experimental parameters, the maximal squeezing factor, which can reach 40 dB. This squeezing factor is far larger than previous ones.

DOI: 10.1103/PhysRevA.89.023838 PACS number(s): 42.50.Dv, 42.50.Pq

I. INTRODUCTION

Spin-squeezing states are quantum correlated states with reduced fluctuations in one of the collective spin components [1–3]. Such states not only play a central role in investigating many-body entanglement [2,4–9], but also have possible applications in atom interferometers and high-precision atom clocks [2,10,11]. Now the preparation of spin-squeezing states has become an important subject in quantum information and quantum metrology [2,3]. In principle, nonlinear spin-spin interactions are necessary for producing spin-squeezing states and, moreover, have been constructed experimentally in both multicomponent Bose-Einstein condensates (BECs) [12–18] and atom-cavity interacting systems [19,20]. However, the generated spin-spin interactions are weak, and thus the corresponding maximal squeezing factors (MSFs) acquired are lower than 10 dB [2,3]. Recently, many proposals [21–30] have been suggested to enhance the upper limits of the MSFs in laboratory conditions, but the experimental challenges are difficult.

Here we present an experimentally feasible method to achieve a large and tunable spin squeezing when an ensemble of many four-level atoms interacts simultaneously with a single-mode photon and classical driving lasers. Recently, a similar setup has been considered experimentally in a BEC-cavity system, and a remarkable quantum phase transition, from a normal phase to a superradiant phase of the Dicke model, was observed [31,32]. The distinct advantage of this setup is that the realized Dicke model has a tunable collective atom-photon coupling through manipulating the intensities of the classical driving lasers [33].

The central idea of our work is to simply introduce a time-dependent collective atom-photon coupling in the realized Dicke model. We show that the MSF can be well controlled by both its driving magnitude and driving frequency. In particular, when increasing the driving magnitude, the MSF increases, in contrast to the known results of the undriven Dicke model [2], and thus can be enhanced rapidly. In the high-frequency approximation, we demonstrate explicitly that this spin squeezing arises from a strong repulsive spin-spin interaction induced by the time-dependent collective atom-photon coupling (for the undriven Dicke model, only a weak attractive spin-spin interaction is generated). Finally, we evaluate analytically, using current experimental parameters [31,32], the MSF, which can reach 40 dB. This MSF is far larger than previous ones [12–20].

II. MODEL AND HAMILTONIAN

Figure 1(a) shows our proposed experimental setup in which an ensemble of many four-level atoms interacts simultaneously with a single-mode photon of the optical cavity and a pair of classical driving lasers. Each atom has two stable ground states, labeled respectively by $|G_1\rangle$ and $|G_2\rangle$, which are coupled through a pair of Raman channels, as shown in Fig. 1(b). The photon, with the creation and annihilation operators $a^\dagger$ and a, mediates the $|G_1\rangle \longleftrightarrow |1\rangle$ and $|G_2\rangle \longleftrightarrow |2\rangle$ transitions, with atom-photon coupling strengths g_1 and g_2, whereas the classical driving lasers induce the $|G_1\rangle \longleftrightarrow |2\rangle$ and $|G_2\rangle \longleftrightarrow |1\rangle$ transitions, with Rabi frequencies Ω_1 and Ω_2.

In the large-detuning limit, the excited states of the atoms can be eliminated adiabatically, and thus an effective two-level system, with the collective spin operators $S_x = \sum_i (|G_2\rangle_{ii}\langle G_1| + |G_1\rangle_{ii}\langle G_2|)$ and $S_z = \sum_i (|G_2\rangle_{ii}\langle G_2| - |G_1\rangle_{ii}\langle G_1|)$, can be constructed. When the parameters are

*chengang971@163.com
†tjia@sxu.edu.cn
‡fnori@riken.jp

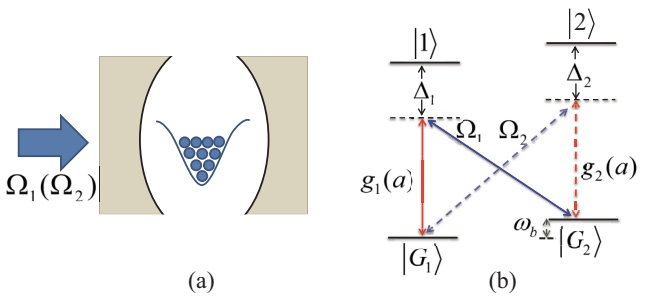

FIG. 1. (Color online) (a) Proposed experimental setup. (b) The atom energy levels are driven simultaneously by a single-mode photon of the optical cavity and a pair of classical driving lasers.

chosen as [33]

$$\frac{g_1^2}{\Delta_1} = \frac{g_2^2}{\Delta_2}, \quad \frac{g_1\Omega_1}{\Delta_1} = \frac{g_2\Omega_2}{\Delta_2}, \tag{1}$$

we realize a Dicke-like Hamiltonian [34]

$$H = \Delta_p a^\dagger a + \omega_0 S_z + \frac{g}{\sqrt{N}}(a^\dagger + a)S_x. \tag{2}$$

In the Hamiltonian (2), the effective cavity frequency $\Delta_p = \delta_c + Ng_1^2/\Delta_1$, where $\delta_c = \omega_c - (\omega_{l2} - \omega_b')$, N is the number of atoms, ω_c is the real cavity frequency, $\omega_b' = (\omega_{l2} - \omega_{l1})/2$ is a frequency close to the frequency ω_b of energy level $|G_2\rangle$, ω_{l1} and ω_{l2} are the driving frequencies of the classical lasers, respectively, and Δ_1 is the detuning. This effective cavity frequency Δ_p varies from $-$GHz to GHz, and even goes beyond this regime. However, when $\Delta_p < 0$, the system becomes unstable [31,32]. Thus, hereafter we consider $\Delta_p \geqslant 0$. The effective atom frequency $\omega_0 = (\omega_b - \omega_b')$, which is of the order of several hundred kHz. The collective atom-photon coupling strength $g = \sqrt{N}g_1\Omega_1/\Delta_1$, which can reach the order of a GHz by independently manipulating the intensities of the classical driving lasers.

III. SPIN SQUEEZING

This four-level model has been regarded as a promising candidate to produce both field squeezing and spin squeezing. For example, two-mode field squeezing [35] and unconditional two-mode squeezing of separated atomic ensembles [36] have been considered by introducing two cavities, mediating the $|G_1\rangle \longleftrightarrow |1\rangle$ and $|G_2\rangle \longleftrightarrow |2\rangle$ transitions, respectively. Recently, it has been proposed that spin squeezing can be achieved by designing degenerate ground states $|G_1\rangle$ and $|G_2\rangle$ ($\omega_0 = 0$) [37,38]. In particular, Ref. [38] demonstrated the existence of a collective atomic dark state, decoupled from the cavity mode field. When explicitly constructing this steady dark state, spin squeezing, which is considerably more robust against noise, can be achieved simultaneously [38]. Here, we mainly achieve a large and tunable spin squeezing by considering a time-dependent collective atom-photon coupling strength $g(t)$, and explore its physical consequences.

When the Rabi frequencies of the classical driving lasers are chosen as

$$\Omega_1 = \Omega_2 = \Omega_d \cos(\omega t), \tag{3}$$

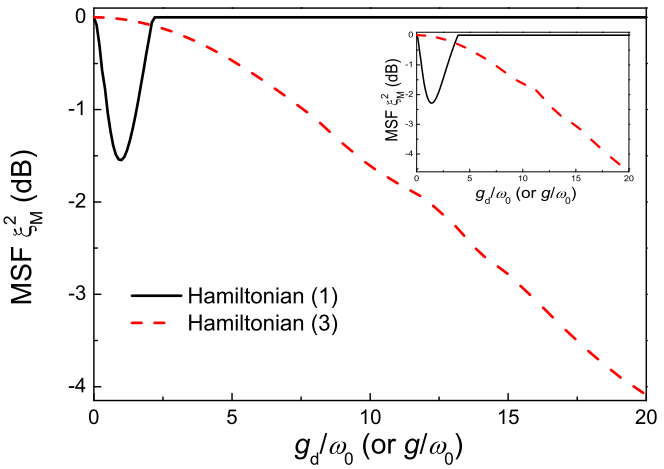

FIG. 2. (Color online) Numerical plot of MSF ξ_M^2 of the undriven Dicke model (2) (black solid curve) and the time-dependent Hamiltonian (5) (red dashed curve) when $N = 10$. Inset shows the MSF ξ_M^2 for $N = 20$. In these figures, the other parameters are chosen as $\Delta_p = \omega_0$ and $\omega = 10\omega_0$.

the collective atom-photon coupling strength becomes

$$g(t) = g_d \cos(\omega t), \tag{4}$$

where $g_d = \sqrt{N}g_1\Omega_d/\Delta_1$ is the effective driving magnitude and ω is the driving frequency. Substituting Eq. (4) into the Hamiltonian (2) yields a time-dependent Dicke model

$$H(t) = \Delta_p a^\dagger a + \omega_0 S_z + \frac{g_d \cos(\omega t)}{\sqrt{N}}(a^\dagger + a)S_x. \tag{5}$$

If the initial state is chosen as

$$|\psi(0)\rangle = \left|S_z = -\frac{N}{2}\right\rangle \otimes |0\rangle, \tag{6}$$

the corresponding squeezing factor is defined as [39]

$$\xi_R^2(t) = \frac{N\Delta S_{\vec{n}_\perp}^2(t)}{|S(t)|^2}, \tag{7}$$

where $\vec{n}_\perp$ refers to an axis, which is perpendicular to the mean-spin direction, $|S| = \sqrt{\langle S_x\rangle^2 + \langle S_y\rangle^2 + \langle S_z\rangle^2}$, and

$$\Delta A^2 = \langle A^2\rangle - \langle A\rangle^2 \tag{8}$$

is the standard deviation. If $|\xi_R^2| < 1$, the state is spin squeezed, and its phase sensitivity, $\Delta\varphi = \xi_R^2/\sqrt{N}$, is improved over the shot-noise limit. In addition, the initial state $|0\rangle$ is a pure state not containing any photons and consequently is not affected by the cavity decay [40,41].

It is very difficult to derive an analytical expression for the squeezing factor of the time-dependent Hamiltonian (5). However, in experiments, the MSF

$$\xi_M^2 = \min\left[\xi_R^2(t)\right] \tag{9}$$

is usually measured [2]. Thus, hereafter we focus mainly on this MSF ξ_M^2. In Fig. 2, we numerically calculate the MSF ξ_M^2 of the undriven Dicke model (2) (black solid curve) and the time-dependent Hamiltonian (5) (red dashed curve), with the same initial state $|\psi(0)\rangle$.

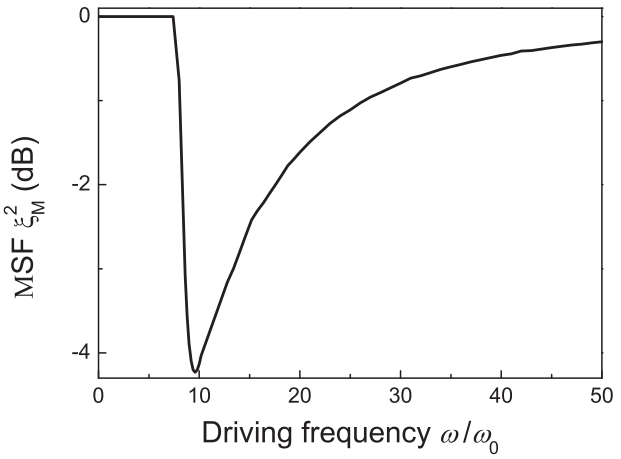

FIG. 3. Numerical plot of MSF ξ_M^2 of the time-dependent Hamiltonian (5) when $g_d = 20\omega_0$ and $N = 10$.

For the undriven Dicke model (2), when increasing the static collective atom-photon coupling g, the MSF ξ_M^2 increases rapidly and then decreases once g goes beyond a critical value g_c. Its physics can be understood as follows: When $g < g_c$, the system is located at the normal phase with no macroscopic collective excitations of both the atoms and the photon, i.e., $\langle a^\dagger a\rangle = 0$. However, this virtual photon acts as a bus and thus generates an attractive spin-spin interaction $-S_x^2$, which can be demonstrated, in the limit when $\Delta_p \gg g$, by second-order perturbation theory [42–45]. Moreover, the interaction strength depends on g^2/Δ_p. Thus, when increasing a weak g, the MSF ξ_M^2 increases. When $g > g_c$, the undriven Dicke model exhibits a strong atom-photon interaction. When increasing g, the atoms and the photon become more and more entangled, and the spin squeezing is suppressed. In particular, in the limit when $g \gg \{\Delta_p, \omega_0\}$, this atom-photon interaction plays a dominate role in the quantum dynamics of the undriven Dicke model. For the given initial state $|\psi(0)\rangle$, we have

$$S_z(t) = \frac{N}{2}\cos(Cgt), \tag{10}$$

where $C = a^\dagger + a$, and thus

$$\xi_R^2(t) = 0. \tag{11}$$

This result agrees well with the direct numerical calculation, as shown by the black solid curve of Fig. 2.

For the time-dependent Hamiltonian (5), the MSF ξ_M^2 exhibits some surprising behavior. As shown by the red dashed curve of Fig. 2, the MSF ξ_M^2 can be largely enhanced by increasing the driving magnitude g_d, which is in contrast to the results of the undriven Dicke model. In Fig. 3, we numerically plot the MSF ξ_M^2 as a function of the driving frequency ω. We find that the MSF ξ_M^2 can also be enhanced by choosing a proper driving frequency ω. In the high-frequency regime, the MSF ξ_M^2 decreases when increasing the driving frequency ω. The above predictions imply that a large MSF can be prepared by controlling the time-dependent collective atom-photon coupling $g(t)$ in experiments.

IV. g_d-INDUCED STRONG REPULSIVE SPIN-SPIN INTERACTION

We now illustrate the fundamental physics that explains why this surprising behavior of spin squeezing can occur in the driven Dicke model. In general, we cannot extract the interesting physics for any driving frequency ω. Fortunately, in the high-frequency approximation, we will demonstrate explicitly that the time-dependent collective atom-photon coupling gives rise to a magnitude-dependent repulsive spin-spin interaction, which is essential for producing spin squeezing. This result is quite different from that of the undriven Dicke model, in which only a weak attractive spin-spin interaction is generated by the static collective coupling.

We first employ a time-dependent unitary transformation

$$U(t) = \exp[-i\chi\sin(\omega t)(a^\dagger + a)S_x], \tag{12}$$

with

$$\chi = \frac{g_d}{\omega\sqrt{N}}, \tag{13}$$

to rewrite the time-dependent Hamiltonian (5) as

$$H_u(t) = U^\dagger(t)H(t)U(t) - iU^\dagger(t)\frac{\partial U(t)}{\partial t}. \tag{14}$$

After a straightforward calculation, we have

$$\begin{aligned} H_u(t) = {} & \Delta_p\left[a^\dagger a + i\chi\sin(\omega t)(-a^\dagger + a)S_x + \chi^2\sin^2(\omega t)S_x^2\right] \\ & + \omega_0\{S_z\cos[\chi\sin(\omega t)(a^\dagger + a)] \\ & + S_y\sin[\chi\sin(\omega t)(a^\dagger + a)]\}. \end{aligned} \tag{15}$$

In addition, for a given quantum state $|\psi(t)\rangle$ of the Hamiltonian (5), the time-dependent quantum state of the Hamiltonian (14) is written as

$$|\psi_u(t)\rangle = U(t)\,|\psi(t)\rangle\,. \tag{16}$$

When $t = 0$, $|\psi_u(0)\rangle = U(0)|\psi(0)\rangle = |\psi(0)\rangle$.

By means of the formulas

$$\begin{aligned} \cos[\vartheta\sin(\omega t)] &= J_0(\vartheta) + 2\sum_{m=1}^{\infty} J_{2m}(\vartheta)\cos(2m\omega t), \\ \sin[\vartheta\sin(\omega t)] &= 2\sum_{m=1}^{\infty} J_{2m+1}(\vartheta)\sin[(2m+1)\omega t], \end{aligned} \tag{17}$$

where $J_0(\cdot)$ and $J_m(\cdot)$ are the zeroth- and integer-order Bessel functions, respectively, the time-dependent Hamiltonian (15) is rewritten as

$$H_u(t) = \sum_{n=-\infty}^{\infty} h_n\exp(in\omega t), \tag{18}$$

where

$$h_{-1} = \omega_0 J_1\left[\frac{g_d(a^\dagger + a)}{\sqrt{N}\omega}\right]S_y - \frac{\Delta_p g_d(a - a^\dagger)S_x}{2\sqrt{N}\omega}, \tag{19}$$

$$h_0 = \Delta_p a^\dagger a + \omega_0 J_0\left[\frac{g_d(a^\dagger + a)}{\sqrt{N}\omega}\right]S_z + \frac{\Delta_p g_d^2 S_x^2}{2N\omega^2}, \tag{20}$$

$$h_1 = \frac{\Delta_p g_d(a - a^\dagger)S_x}{2\sqrt{N}\omega} + \omega_0 J_1\left[\frac{g_d(a^\dagger + a)}{\sqrt{N}\omega}\right]S_y. \tag{21}$$

The other expressions for h_n ($n \geqslant 2$) are too complicated to list here.

In the high-frequency approximation ($\omega \gg \{\Delta_p, \omega_0\}$) [46], we neglect all the time-dependent terms in the Hamiltonian (18), in analogy with the standard rotating-wave approximation, and then obtain an effective time-independent Hamiltonian

$$H_e = \frac{q}{N} S_x^2 + \Delta_p a^\dagger a + \omega_0 J_0 \left[\frac{g_d}{\sqrt{N}\omega}(a^\dagger + a)\right] S_z, \qquad (22)$$

where

$$q = \frac{\Delta_p g_d^2}{2\omega^2}. \qquad (23)$$

The Hamiltonian (22) shows clearly that the time-dependent collective atom-photon coupling induces a repulsive spin-spin interaction ($q > 0$ for $\Delta_p > 0$), which can be controlled widely and independently by tuning the effective cavity frequency Δ_p and, especially, the driving magnitude g_d and the driving frequency ω.

We emphasize that for the undriven Dicke model, the attractive spin-spin interaction $-S_x^2$ is mediated by a virtual photon. As a result, its interaction strength is weak, and can be derived from second-order perturbation theory when $\Delta_p \gg g$ [42–45]. However, the repulsive spin-spin interaction realized here arises from the driving photon under the high-frequency approximation, which needs to satisfy the following condition: $\omega \gg \{\Delta_p, \omega_0\}$ (the condition $\Delta_p \gg g$ in the undriven Dicke model is now relaxed). This means that the driving magnitude g_d can reach the same order as the driving frequency ω and go beyond the effective cavity frequency Δ_p. Thus, the corresponding interaction strength can reach a large value. For example, when the parameters are chosen as $g_d = \omega = 2\pi \times 0.5$ GHz and $\Delta_p = 0.1\omega = 2\pi \times 0.05$ GHz, then the repulsive spin-spin interaction strength becomes $q = \Delta_p g_d^2/(2\omega^2) = 2\pi \times 250$ MHz, which is 2 to 3 orders larger than that of the undriven Dicke model [19,20].

In order to further reveal the role of the generated repulsive spin-spin interaction q, in Fig. 4, we numerically compare the MSF ξ_M^2 of the time-dependent Hamiltonian (5) with that of the effective time-independent Hamiltonian (22). These results imply that the spin squeezing of the time-dependent Hamiltonian (5) for the initial state $|\psi(0)\rangle$ can be well described by the effective Hamiltonian (22) in the high-frequency approximation. That is, we can employ the effective time-independent Hamiltonian (22) to analyze the predictions in Figs. 2 and 3.

It should be remarked that, for the time-independent Hamiltonian (22), there also exists a weak photon-induced spin-spin interaction in the z direction, apart from the repulsive spin-spin interaction qS_x^2/N. However, when the initial state is chosen as $|\psi(0)\rangle = |S_z = -N/2\rangle \otimes |0\rangle$, this photon-induced spin-spin interaction has almost no role in producing spin squeezing. This means that the repulsive spin-spin interaction is central for producing spin squeezing in the time-dependent Hamiltonian (5), with the initial state $|\psi(0)\rangle$. When increasing the driving magnitude g_d, this repulsive spin-spin interaction q increases and reaches a large value. This strong repulsive spin-spin interaction q can significantly enhance the MSF ξ_M^2, as shown by the red dashed curve of Fig. 2. However, when increasing the driving frequency ω, the repulsive spin-spin interaction q becomes weaker and, correspondingly, the MSF ξ_M^2 decreases, as shown in Fig. 3.

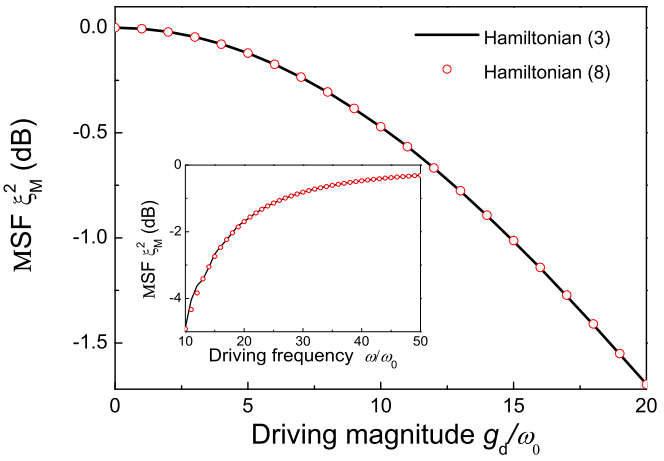

FIG. 4. (Color online) Numerical plot of MSF ξ_M^2 as a function of the driving magnitude g_d, when $\omega = 20\omega_0$ and $N = 10$. Inset shows MSF ξ_M^2 versus driving frequency ω, when $g_d = 20\omega_0$ and $N = 10$. In these figures, the black solid curves denote the results of the time-dependent Hamiltonian (5) and the red open symbols correspond to the results of the effective time-independent Hamiltonian (22).

V. A LARGE SQUEEZING FACTOR IN EXPERIMENTS

In this section, we evaluate the MSF ξ_M^2 by considering current experimental parameters, especially with a large atom number. For a large atom number $N \sim 10^4$, the MSF ξ_M^2 is hard to obtain numerically. Fortunately, in such a case, we have $g_d/(\sqrt{N}\omega) \to 0$. This implies that the effective time-independent Hamiltonian (22) becomes

$$H_e = \frac{q}{N} S_x^2 + \omega_0 S_z. \qquad (24)$$

When $\omega_0 \gg q/N$, the MSF ξ_M^2 for the Hamiltonian (24) can be derived explicitly from the frozen-spin approximation [2].

In terms of the Heisenberg equation of motion, we obtain

$$\begin{aligned} \dot{S}_x &= -\omega_0 S_y, \\ \dot{S}_y &= -\frac{q}{N}(S_z S_x + S_x S_z) + \omega_0 S_x. \end{aligned} \qquad (25)$$

For the given initial state $|\psi(0)\rangle = |S_z = -\frac{N}{2}\rangle$, $\langle S_y(0)\rangle = \langle S_x(0)\rangle = 0$, and $\langle S_y^2(0)\rangle = \langle S_x^2(0)\rangle = N/4$. In general, the differential equations (25) cannot be solved analytically. However, when $\omega_0 \gg q/N$, $2\langle S_z(t)\rangle/N$ remains approximately unchanged under the initial state $|\psi(0)\rangle$, as shown in Fig. 5. This implies that we can make an approximation by replacing S_z by $-N/2$, which leads to the harmonic solutions

$$\begin{aligned} S_x(t) &\simeq S_x(0)\cos(\eta t) + \frac{\omega_0}{\eta} S_y(0)\sin(\eta t), \\ S_y(t) &\simeq S_y(0)\cos(\eta t) - \frac{\eta}{\omega_0} S_x(0)\sin(\eta t), \end{aligned} \qquad (26)$$

where

$$\eta = \sqrt{\omega_0(\omega_0 + q)}. \qquad (27)$$

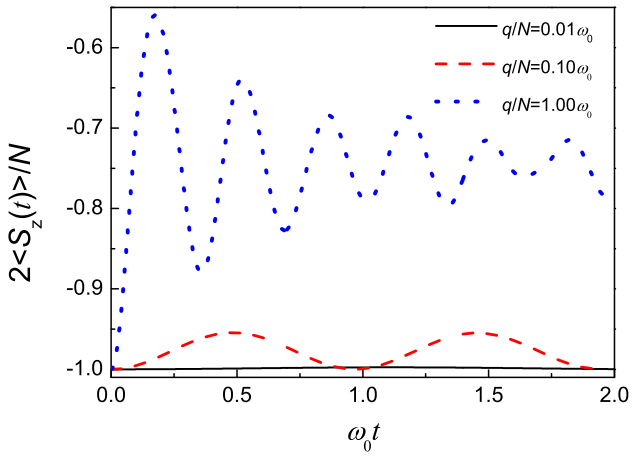

FIG. 5. (Color online) Quantum dynamics of $2\langle S_z(t)\rangle/N$ for the different spin-spin interaction strengths: $q/N = 0.01\omega_0$,$q/N = 0.1\omega_0$, and $q/N = \omega_0$, when $N = 100$.

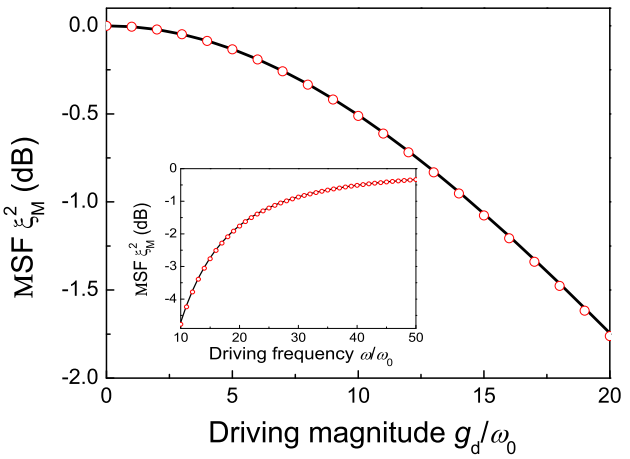

FIG. 6. (Color online) The MSF $\xi^2_{\rm M}$ as a function of the driving magnitude g_d, when $\omega = 20\omega_0$ and $N = 100$. Inset shows MSF $\xi^2_{\rm M}$ versus the driving frequency ω, when $g_d = 20\omega_0$ and $N = 10$. In these figures, the black solid curves denote the direct numerical calculation of the effective time-independent Hamiltonian (24), and the red open symbols correspond to the analytical results in Eq. (31).

Based on Eq. (26), we have

$$\Delta S_x^2(t) = \frac{N}{4}\left[\cos^2(\eta t) + \frac{\omega_0^2}{\eta^2}\sin^2(\eta t)\right],$$
$$\Delta S_y^2(t) = \frac{N}{4}\left[\cos^2(\eta t) + \frac{\eta^2}{\omega_0^2}\sin^2(\eta t)\right]. \tag{28}$$

Since $\eta > \omega_0$, the reduced spin fluctuations occur in the x direction, i.e., the definition of spin squeezing, $\xi^2_{\rm R}(t) = N\Delta S^2_{\vec{n}_\perp}(t)/|S(t)|^2$, becomes

$$\xi_x^2(t) = \frac{4\Delta S_x^2(t)}{N}. \tag{29}$$

Substituting the expression $\Delta S_x^2(t)$ in Eq. (28) into Eq. (29) and then choosing

$$t = \frac{(2n+1)\pi}{2\omega}\ (n = 0,1,2,\ldots), \tag{30}$$

the MSF is finally obtained by

$$\xi^2_{\rm M} = \frac{\omega_0^2}{\eta^2} = \frac{1}{1+q/\omega_0}, \tag{31}$$

which agrees with the direct numerical calculation, as shown in Fig. 6.

It can be seen from Eq. (31) that, when increasing the driving magnitude g_d, the MSF $\xi^2_{\rm M}$ increases (red dashed curve in Fig. 2), but decreases when increasing the driving frequency ω (Fig. 3). In addition, Eq. (31) also shows that the MSF $\xi^2_{\rm M}$ is independent of atom number N. In fact, the value of the atom number N restricts the upper limits of the repulsive spin-spin interaction strength q, since Eq. (31) is valid for $q \ll N\omega_0$. When $N = 10^4$, we approximately take $q = 10^3\omega_0$, which becomes $q = 10^4\omega_0$ when $N = 10^5$. This means that, using current experimental parameters with $N = 10^5$, the MSF reaches 40 dB (30 dB for $N = 10^4$). When $\omega_0 \sim q/N$ or $\omega_0 < q/N$, the analytical expression in Eq. (31) is invalid. However, with decreasing ω_0, the MSF increases [2,3].

In multicomponent BECs, the spin-spin interactions can also be realized by controlling the direct atom-atom collision interactions. In principle, this effective spin-spin interaction can be tuned by a magnetic-field-dependent Feshbach resonant technique [47]. However, similar to the result of the undriven Dicke model, its strength is also weak (from kHz to MHz) and is far smaller than our prediction ($\sim$ several hundred MHz). As a result, the generated MSF is also far smaller than our result (40 dB).

VI. POSSIBLE EXPERIMENTAL OBSERVATIONS

Here we briefly discuss how to possibly observe these results in experiments. As an example, we consider the D_2 line of ^{87}Rb. The two stable ground states, $|G_1\rangle$ and $|G_2\rangle$ in our proposal, are chosen as two hyperfine substates of $5S_{1/2}$, i.e., $|F = 1, m_F = -1\rangle = |G_1\rangle$ and $|F = 2, m_F = 2\rangle = |G_2\rangle$, with a splitting $\sim 2\pi \times 6.8$ GHz; whereas the virtual excited states $|1\rangle$ and $|2\rangle$ can be chosen as two of the hyperfine substates in the $5P_{1/2}$ excited state. The decay rates for the $5P_{1/2}$ excited state and the photon are given by $\gamma = 2\pi \times 3$ MHz and $\kappa = 2\pi \times 1.3$ MHz, respectively [48].

In addition, by controlling the frequency ω_b', which is close to the frequency ω_b of the energy level $|G_2\rangle$, the effective atom frequency is of the order of several hundred kHz. Moreover, the repulsive spin-spin interaction strength q can be of the order of a GHz by independently manipulating the intensities of the classical driving lasers. For example, when the parameters are chosen as $g_d = \omega = 2\pi \times 0.5$ GHz and $\Delta_p = 0.1\omega = 2\pi \times 0.05$ GHz, then $q = \Delta_p g_d^2/(2\omega^2) = 2\pi \times 250$ MHz. Therefore, the condition $q = 10^4\omega_0$ for achieving the MSF $\xi^2_{\rm M} = 40$ dB can be satisfied. Moreover, the shortest time for generating the MSF is $t = \pi/(2\omega) = 0.5$ ns $\ll \tau_a = 1/\gamma = 53$ ns. This means that the large spin squeezing can be well realized within the atom decay time τ_a.

VII. CONCLUSIONS

In summary, we have presented an experimentally feasible method to achieve a large and tunable spin squeezing by introducing a time-dependent collective atom-photon coupling. We have demonstrated explicitly, in the high-frequency approximation, that this spin squeezing arises from the strong repulsive spin-spin interaction induced by the time-dependent collective atom-photon coupling. More importantly, using current experimental parameters with $N = 10^5$, we have derived a large MSF of about 40 dB. We believe that these results could have applications in quantum information and quantum metrology.

ACKNOWLEDGMENTS

We thank Professor Su Yi, and Dr. Qifeng Liang, Dr. Jian Ma, and Dr. Y.G. Deng for their useful comments. This work was supported partly by the 973 program under Grant No. 2012CB921603; the NNSFC under Grant No. 61275211; the PCSIRT under Grant No. IRT13076; the NCET under Grant No. 13-0882; the FANEDD under Grant No. 201316; and the ZJNSF under Grant No. LY13A040001. F.N. is partially supported by the RIKEN iTHES Project; MURI Center for Dynamic Magneto-Optics; Grant-in-Aid for Scientific Research (S); MEXT Kakenhi on Quantum Cybernetics; and the JSPS via its FIRST program.

[1] M. Kitagawa and M. Ueda, Phys. Rev. A **47**, 5138 (1993).
[2] J. Ma, X. Wang, C. P. Sun, and F. Nori, Phys. Rep. **509**, 89 (2011).
[3] N. P. Robins, P. A. Altin, J. E. Debs, and J. D. Close, Phys. Rep. **529**, 265 (2013).
[4] L.-M. Duan, A. Sørensen, J. I. Cirac, and P. Zoller, Phys. Rev. Lett. **85**, 3991 (2000).
[5] A. Sørensen, L.-M. Duan, J. I. Cirac, and P. Zoller, Nature (London) **409**, 63 (2001).
[6] J. K. Korbicz, J. I. Cirac, and M. Lewenstein, Phys. Rev. Lett. **95**, 120502 (2005).
[7] G. Tóth, C. Knapp, O. Guhne, and H. J. Briegel, Phys. Rev. A **79**, 042334 (2009).
[8] O. Gühne and G. Tóth, Phys. Rep. **474**, 1 (2009).
[9] R. J. Sewell, M. Koschorreck, M. Napolitano, B. Dubost, N. Behbood, and M. W. Mitchell, Phys. Rev. Lett. **109**, 253605 (2012).
[10] G. Santarelli, P. Laurent, P. Lemonde, A. Clairon, A. G. Mann, S. Chang, A. N. Luiten, and C. Salomon, Phys. Rev. Lett. **82**, 4619 (1999).
[11] K. Hammerer, A. S. Sørensen, and E. S. Polzik, Rev. Mod. Phys. **82**, 1041 (2010).
[12] J. Estève, C. Gross, A. Weller, S. Giovanazzi, and M. K. Oberthaler, Nature (London) **455**, 1216 (2008).
[13] C. Gross, T. Zibold, E. Nicklas, J. Estève, and M. K. Oberthaler, Nature (London) **464**, 1165 (2010).
[14] M. F. Riede, P. Böhi, Y. Li, T. W. Hänsch, A. Sinatra, and P. Treutlein, Nature (London) **464**, 1170 (2010).
[15] E. M. Bookjans, C. D. Hamley, and M. S. Chapman, Phys. Rev. Lett. **107**, 210406 (2011).
[16] B. Lücke, M. Scherer, J. Kruse, L. Pezz, F. Deuretzbacher, P. Hyllus, O. Topic, J. Peise, W. Ertmer, J. Arlt, L. Santos, A. Smerzi, and C. Klempt, Science **334**, 773 (2011).
[17] C. D. Hamley, C. S. Gerving, T. M. Hoang, E. M. Bookjans, and M. S. Chapman, Nat. Phys. **8**, 305 (2012).
[18] M. J. Martin, M. Bishof, M. D. Swallows, X. Zhang, C. Benko, J. von-Stecher, A. V. Gorshkov, A. M. Rey, and J. Ye, Science **341**, 632 (2013).
[19] I. D. Leroux, M. H. Schleier-Smith, and V. Vuletić, Phys. Rev. Lett. **104**, 073602 (2010).
[20] Z. Chen, J. G. Bohnet, S. R. Sankar, J. Dai, and J. K. Thompson, Phys. Rev. Lett. **106**, 133601 (2011).
[21] X. Hu and F. Nori, Phys. Rev. Lett. **79**, 4605 (1997).
[22] X. Hu and F. Nori, Phys. B **263-264**, 16 (1999).
[23] A. M. Zagoskin, E. Il'ichev, M. W. McCutcheon, J. F. Young, and F. Nori, Phys. Rev. Lett. **101**, 253602 (2008).
[24] C. M. Trail, P. S. Jessen, and I. H. Deutsch, Phys. Rev. Lett. **105**, 193602 (2010).
[25] T. Vanderbruggen, S. Bernon, A. Bertoldi, A. Landragin, and P. Bouyer, Phys. Rev. A **83**, 013821 (2011)
[26] Y. C. Liu, Z. F. Xu, G. R. Jin, and L. You, Phys. Rev. Lett. **107**, 013601 (2011).
[27] B. Juliá-Díaz, T. Zibold, M. K. Oberthaler, M. Melé-Messeguer, J. Martorell, and A. Polls, Phys. Rev. A **86**, 023615 (2012).
[28] A. Z. Chaudhry and J. Gong, Phys. Rev. A **86**, 012311 (2012).
[29] C. Shen and L.-M. Duan, Phys. Rev. A **87**, 051801 (2013).
[30] J. Lian, L. Yu, J.-Q. Liang, G. Chen, and S. Jia, Sci. Rep. **3**, 3166 (2013).
[31] K. Baumann, C. Guerlin, F. Brennecke, and T. Esslinger, Nature (London) **464**, 1301 (2010).
[32] K. Baumann, R. Mottl, F. Brennecke, and T. Esslinger, Phys. Rev. Lett. **107**, 140402 (2011).
[33] F. Dimer, B. Estienne, A. S. Parkins, and H. J. Carmichael, Phys. Rev. A **75**, 013804 (2007).
[34] R. H. Dicke, Phys. Rev. **93**, 99 (1954).
[35] R. Guzmán, J. C. Retamal, E. Solano, and N. Zagury, Phys. Rev. Lett. **96**, 010502 (2006).
[36] A. S. Parkins, E. Solano, and J. I. Cirac, Phys. Rev. Lett. **96**, 053602 (2006).
[37] S. B. Zheng, Phys. Rev. A **86**, 013828 (2012).
[38] E. G. Torre, J. Otterbach, E. Demler, V. Vuletić, and M. D. Lukin, Phys. Rev. Lett. **110**, 120402 (2013).
[39] D. J. Wineland, J. J. Bollinger, W. M. Itano, and D. J. Heinzen, Phys. Rev. A **50**, 67 (1994).
[40] X. Wang, A. Miranowicz, Y. X. Liu, C. P. Sun, and F. Nori, Phys. Rev. A **81**, 022106 (2010).
[41] X. Yin, J. Ma, X. G. Wang, and F. Nori, Phys. Rev. A **86**, 012308 (2012).
[42] S. Morrison and A. S. Parkins, Phys. Rev. Lett. **100**, 040403 (2008); Phys. Rev. A **77**, 043810 (2008).
[43] G. Chen, J.-Q. Liang, and S. Jia, Opt. Exp. **17**, 19682 (2009).
[44] J. Larson, Europhys. Lett. **90**, 54001 (2010).
[45] S. D. Bennett, N. Y. Yao, J. Otterbach, P. Zoller, P. Rabl, and M. D. Lukin, Phys. Rev. Lett. **110**, 156402 (2013).
[46] M. Grifoni and P. Hänggi, Phys. Rep. **304**, 229 (1998).
[47] C. Chin, R. Grimm, P. Julienne, and E. Tiesinga, Rev. Mod. Phys. **82**, 1225 (2010).
[48] F. Brennecke, T. Donner, S. Ritter, T. Bourdel, M. Köhl, and T. Esslinger, Nature (London) **450**, 268 (2007).